

Role of Hypoxia-Inducible Factors in Regulating Right Ventricular Function and Remodeling during Chronic Hypoxia-Induced Pulmonary Hypertension

Kimberly A. Smith, Gregory B. Waypa, V. Joseph Dudley, G.R. Scott Budinger,
Hiam Abdala-Valencia, Elizabeth Bartom, and Paul T. Schumacker

ONLINE DATA SUPPLEMENT

Online Data Supplement

Expanded Materials and Methods

Real time RT-PCR. To confirm deletion of HIF-1 α in cardiomyocytes and smooth muscle cells, total RNA was extracted and column purified from RV and abdominal aortas of SMC HIF-1 α , Myh6Cre HIF-1 α , and SMC-Myh6Cre HIF-1 α mice and their littermate controls using the RNeasy kit (Qiagen, Valencia, CA). Real time RT-PCR was performed in two steps. First-strand cDNA was synthesized using iScript™ Reverse Transcription Supermix (BioRad, Hercules, CA) with random primers. Real time PCR amplification of first-strand cDNA was performed using iQ™ SYBR Green Supermix (BioRad) using the following primers: HIF-1 α forward AGGATGATGTCTGAACGTCGAAA; HIF-1 α reverse GGGGAAGTGGCAACTGATGA; tubulin forward GGAATATGGACTCCGTTTCGC; tubulin reverse CCCAGACTGACCGAAAACGA; beta-2-microglobulin (B2M) forward GGAGAATGGGAAGCCGAACA; B2M reverse CCCGTTCTTCAGCATTGGA.

Chronic hypoxia. Mice were exposed to normoxia (21% O₂) or hypoxia (10% O₂) in the same room for 4 weeks (range: 28-31 days) beginning 2 weeks after the completion of tamoxifen administration. Chronic hypoxia was maintained in a normobaric environmental chamber with continuous monitoring of ambient O₂ and timed air filtration (10 \pm 0.02% O₂, 55% humidity, ~25 °C) (Coy Laboratory Products, Grass Lake, MI). All mice experienced identical light-dark cycling; food and water were accessible *ad libitum*.

Echocardiography. Cardiac function was assessed by echocardiography using a VisualSonics Vevo-770 echo system (VisualSonics, Toronto, Ontario, Canada). Echocardiograms were obtained on lightly anesthetized mice (isofluorane inhalation). Images obtained from the parasternal long axis were used to determine left ventricular ejection fraction, fractional

shortening, stroke volume, cardiac output, right ventricular free wall thickness, and pulmonary acceleration time/ejection time.

Hemodynamics. Hemodynamics were measured on mice anesthetized with avertin (240 mg/kg, ip) and the trachea was cannulated with a 24 gauge catheter. The mice were mechanically ventilated (Harvard Instruments, Holliston, MA, USA) at 150 breaths/min and a tidal volume 200 μ l. Hypoxia-induced changes in right ventricular systolic pressure (RVSP) were assessed by opening the chest cavity and inserting a micro-tip pressure transducer catheter (Millar, Houston, TX, USA) into the right ventricle via apical puncture. Measurements of RVSP in mice housed under normoxia were performed while the mice were ventilated with room air. For mice housed under chronic hypoxia, the ventilator gas was switched to hypoxia (10% O₂, 90% N₂) while RVSP was measured. Two RVSP measurements were performed in each mouse, separated by 2 minutes, and then averaged to obtain a single RVSP for each mouse.

Systemic arterial blood pressure. Mean arterial blood pressure was measured noninvasively using a tail cuff system (CODA System, Kent Scientific, Torrington, CT, USA). Following 3 cycles of acclimation, systolic, diastolic, and mean pressure measurements were taken from awake mice. 10-20 tail occlusion cycles were averaged for each mouse.

Vascular remodeling. Pulmonary vascular remodeling was assessed in lungs which were inflation-fixed with 4% formaldehyde and embedded in paraffin. Tissue blocks were sectioned and stained with hematoxylin and eosin (H&E). Histology services were provided by the Northwestern University Mouse Histology and Phenotyping Laboratory which is supported by NCI P30-CA060553 awarded to the Robert H Lurie Comprehensive Cancer Center. PA wall thickness was assessed by measuring the cross-sectional area of pulmonary arteries and subtracting the cross-sectional area of the lumen. PA wall thickness was normalized to vessel diameter using Image J (NIH, Bethesda, MD, USA).

Fulton's index. To measure the Fulton's index, hearts were removed from mice and the right ventricle was dissected from the left ventricle and septum. The Fulton's index was calculated as a ratio of the weight of the right ventricle to the weight of the left ventricle plus septum.

Cardiomyocyte diameter. To measure the cardiomyocyte diameter, formalin-fixed paraffin embedded hearts were transversely sectioned and stained with Wheat Germ Agglutinin (WGA, Molecular Probes, Eugene, OR, USA). Cardiomyocyte diameter in the RV was measured using Image J.

Statistics. Changes in RVSP, Fulton's Index, and PA remodeling were analyzed using two-way ANOVA with post-hoc analysis using Sidak's multiple comparisons test. Statistical significance was set $p < 0.05$.

RNA-Seq analysis. Freshly harvested RV tissue was shredded to disrupt the cells (QIAshredder catalog no. 79656, QIAGEN) and total RNA was isolated (RNeasy mini kit, catalog no. 74104, QIAGEN). RNA concentration and quality were tested using TapeStation 4200 (Agilent), all samples had RIN over 8.0. RNA-seq libraries were generated using a NEB Next RNA Ultra library preparation kit with poly(A) enrichment module from 500 ng of total RNA. RNA-seq-ready libraries were pooled and sequenced on a NextSeq 500 instrument (Illumina) using High Output 75 cycles V2 kit to the average depth of 10M reads per sample. Sequencing data were processed using the modular pipeline Ceto using "Genomics Nodes" and "Analytics Nodes" on Quest, Northwestern University's High-Performance Computing Cluster. Briefly, the data were demultiplexed using bcl2fastq (Illumina), after FastQC assessment, trimming with trimmomatic, the reads were mapped using TopHat2 to the mm10 reference genome and reads were quantified using htseq2. Differential gene expression analysis was performed using the EdgeR statistical package.

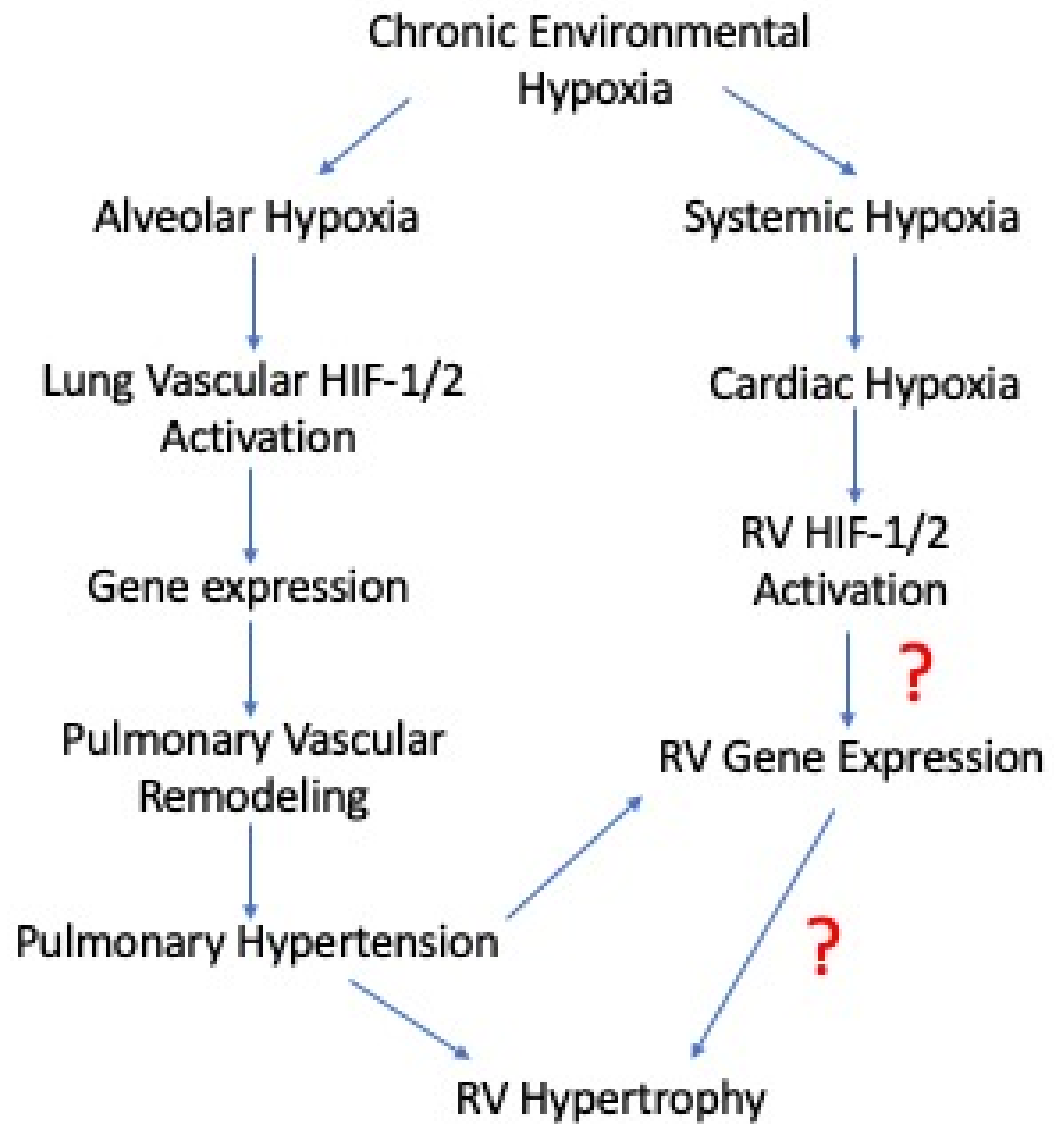
Supplementary Figure Legends

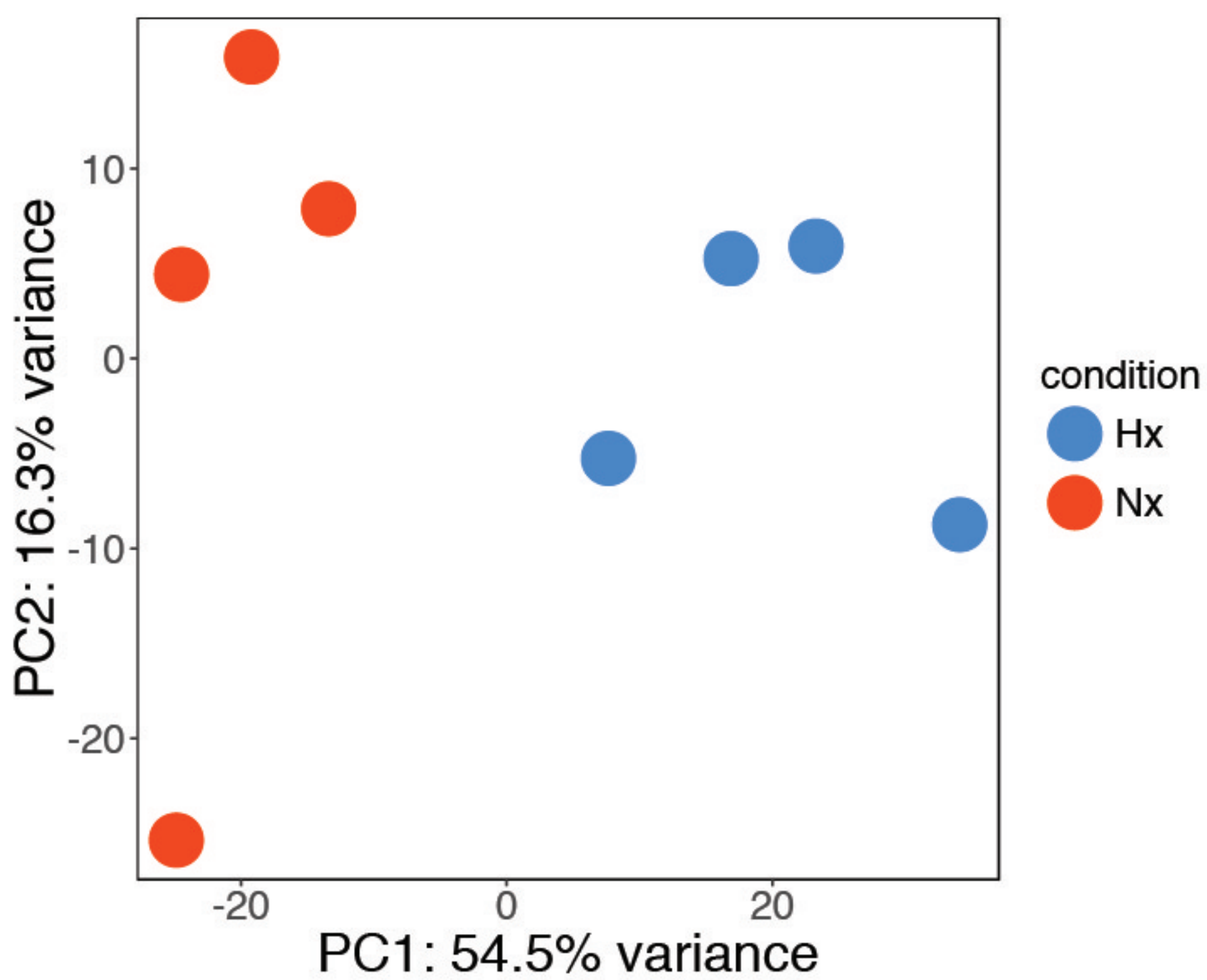
Suppl. Fig. E1: Hypothesized effect of chronic hypoxia on HIF-1 and/or HIF-2 in the RV, and the possible roles of these transcription factors on RV hypertrophy.

Suppl. Figure E2: Principal component analysis of differential gene expression reveals significant effects of chronic hypoxia in wild type (WT) compared with cardiac HIF-1 α and/or HIF-2 α knockout mice (n=4 in each group).

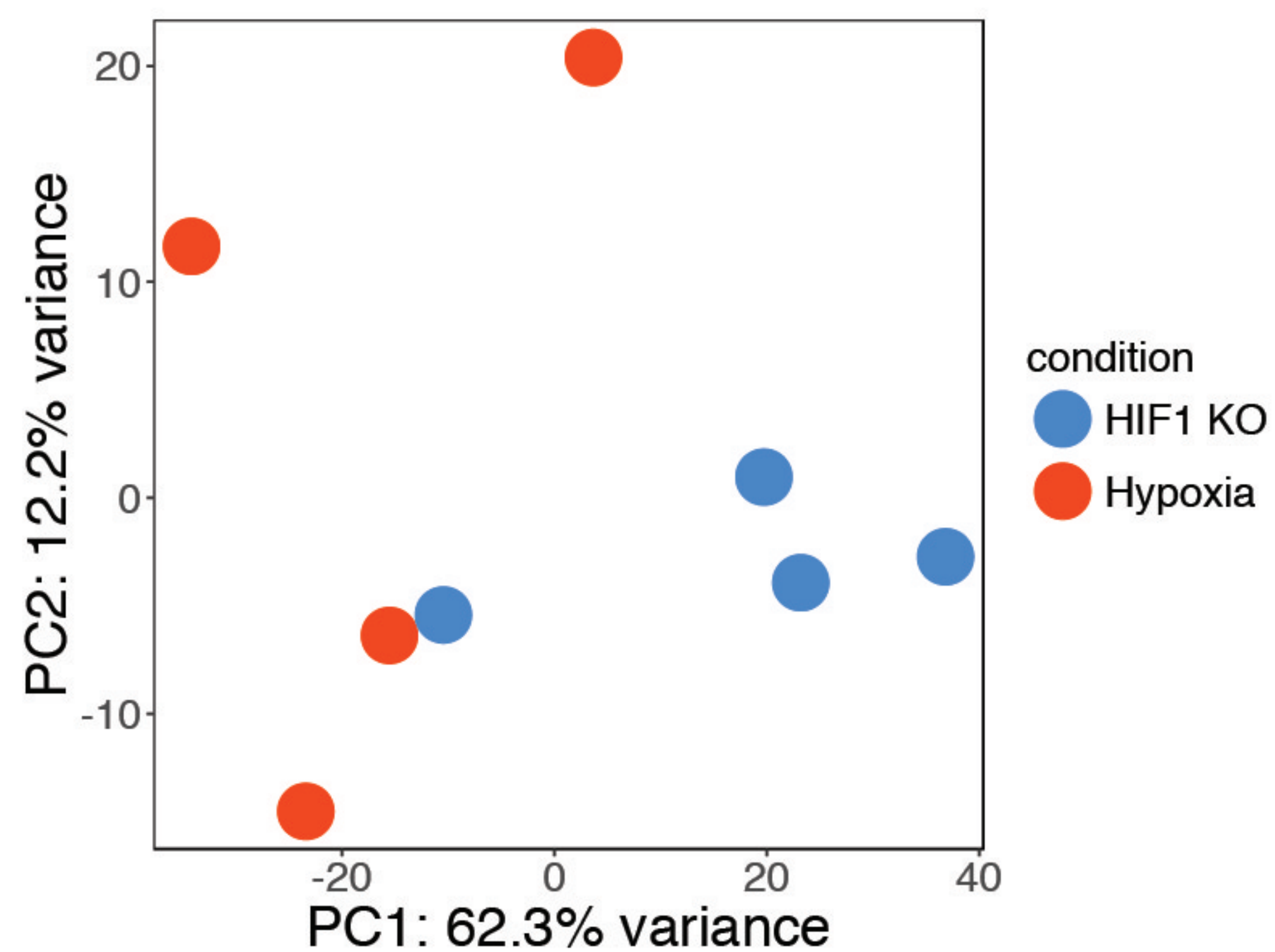
Suppl. Figure E3: Venn diagram depiction of the differential gene expression in response to chronic hypoxia in wild type and HIF-1 α and/or HIF-2 α knockout mice showing that HIF-1 and HIF-2 regulate largely independent gene sets, and that some responses to chronic hypoxia are HIF-independent (n=4 in each group).

Suppl. Figure E4. Conceptual summary of the results indicating that HIF-1 activation in the RV during chronic hypoxia helps to lessen hypertrophic remodeling, whereas HIF-2 does not.

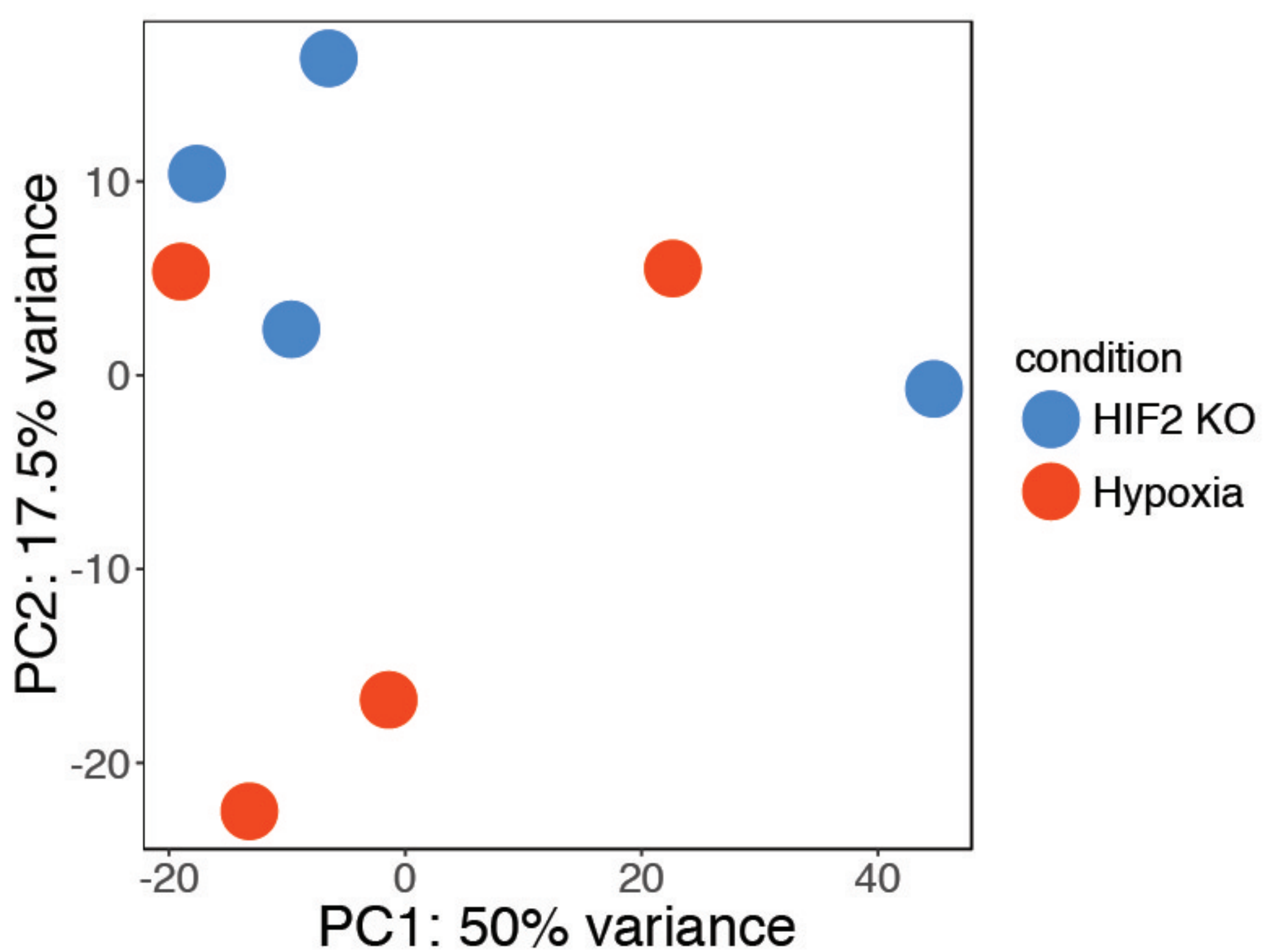




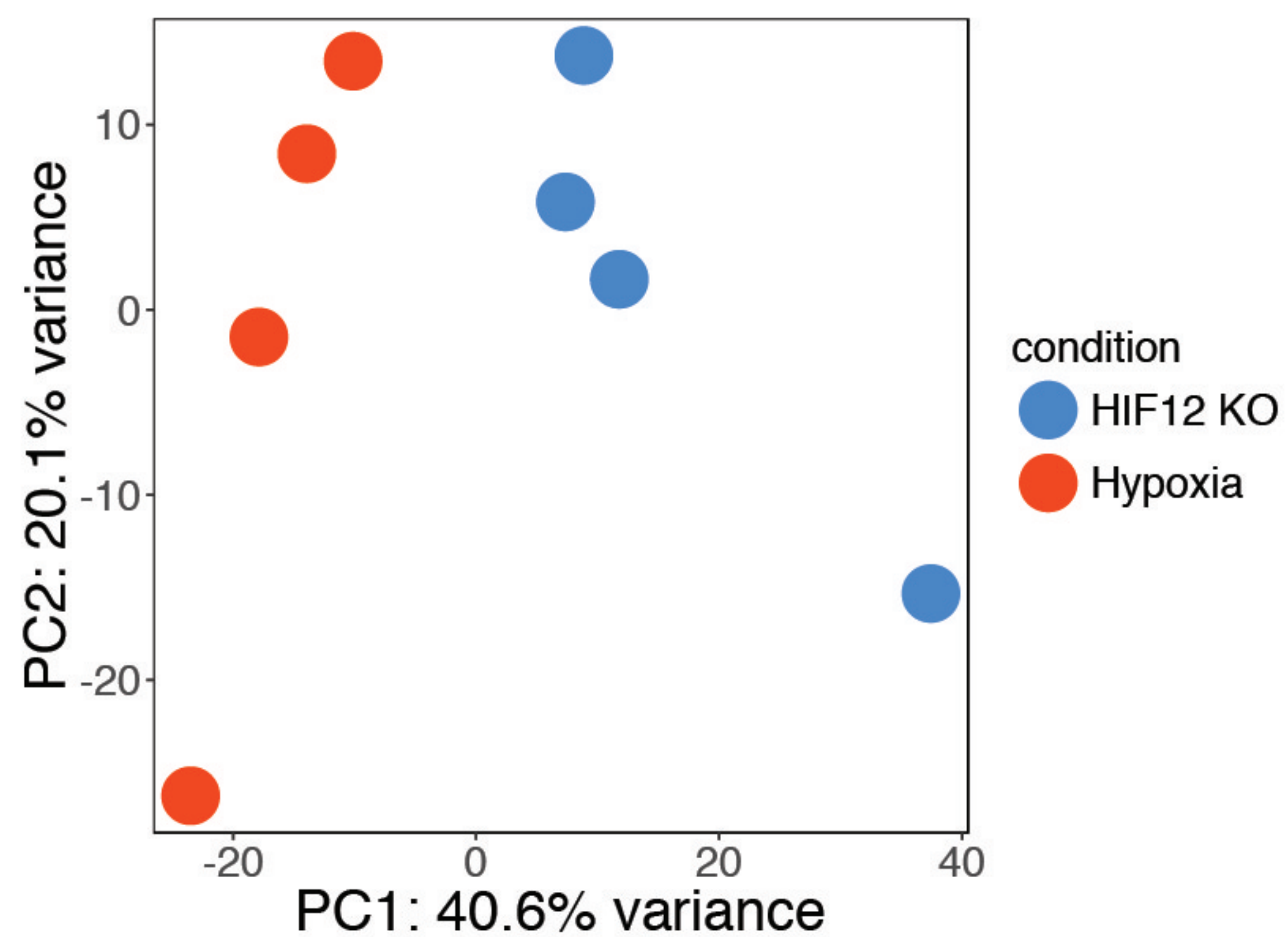
WT Normoxia vs. Hypoxia



Hypoxia: WT vs HIF-1 KO



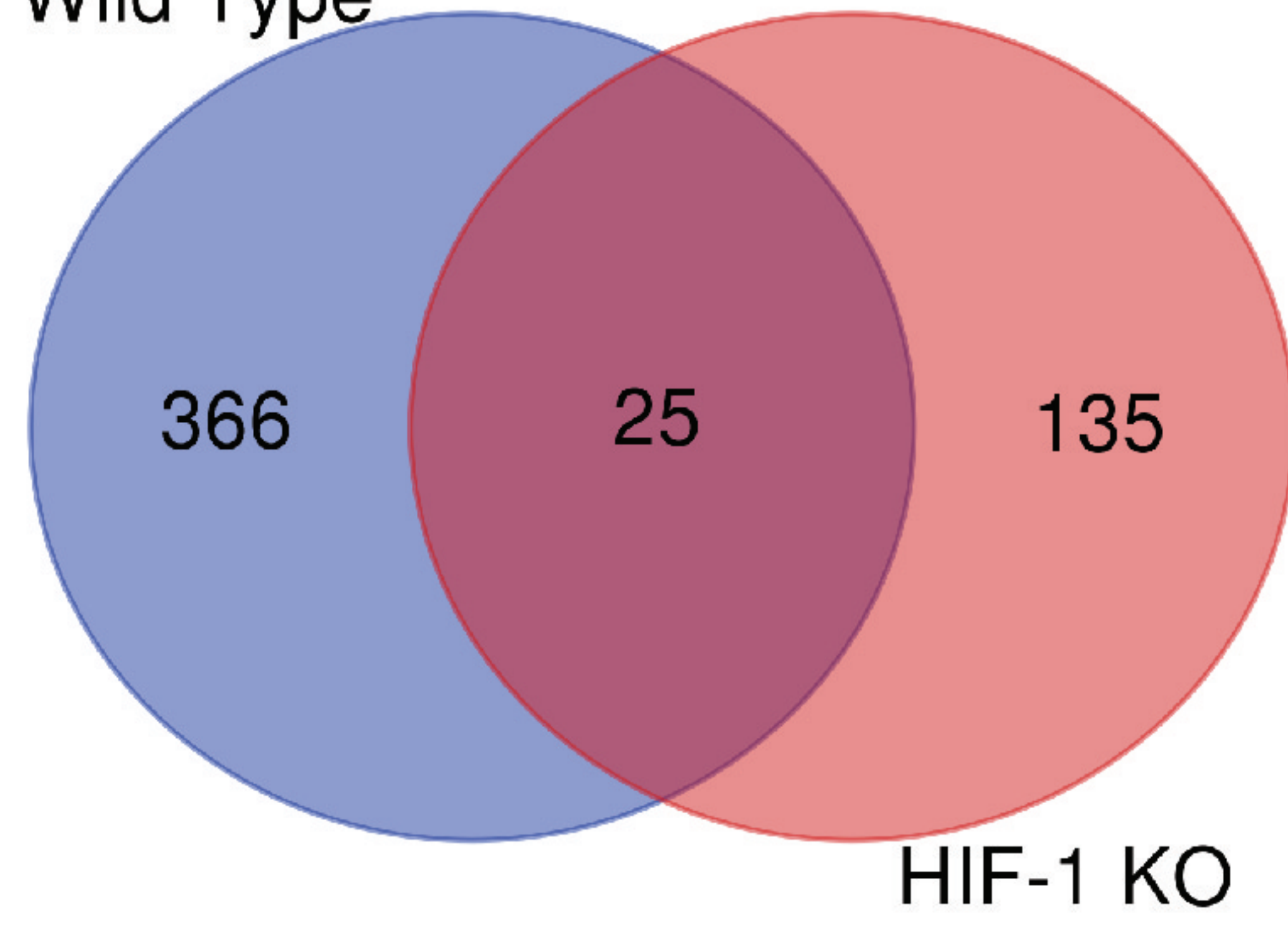
Hypoxia: WT vs. HIF-2 KO



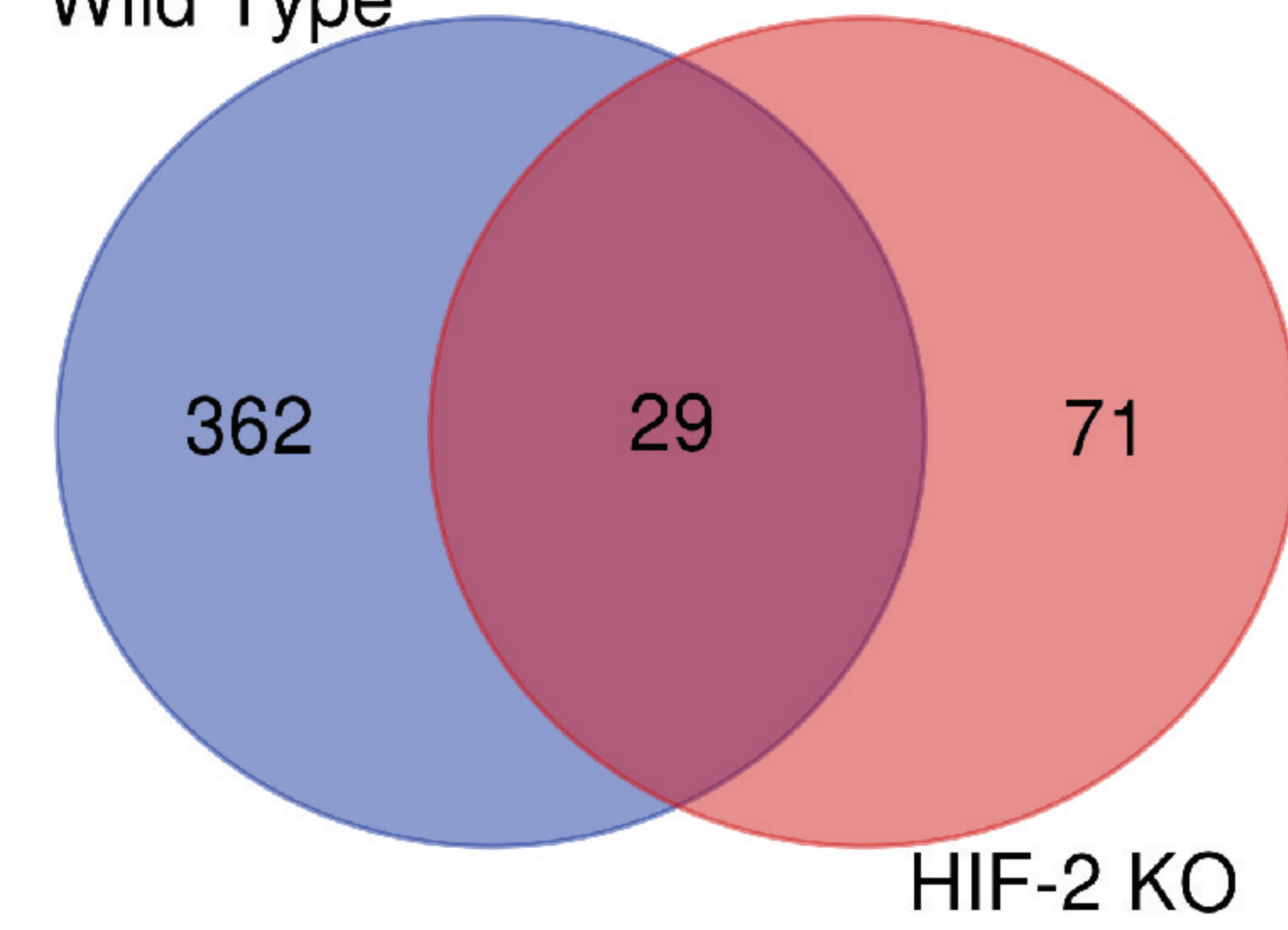
Hypoxia: WT vs. HIF1/2 KO

Chronic Hypoxia

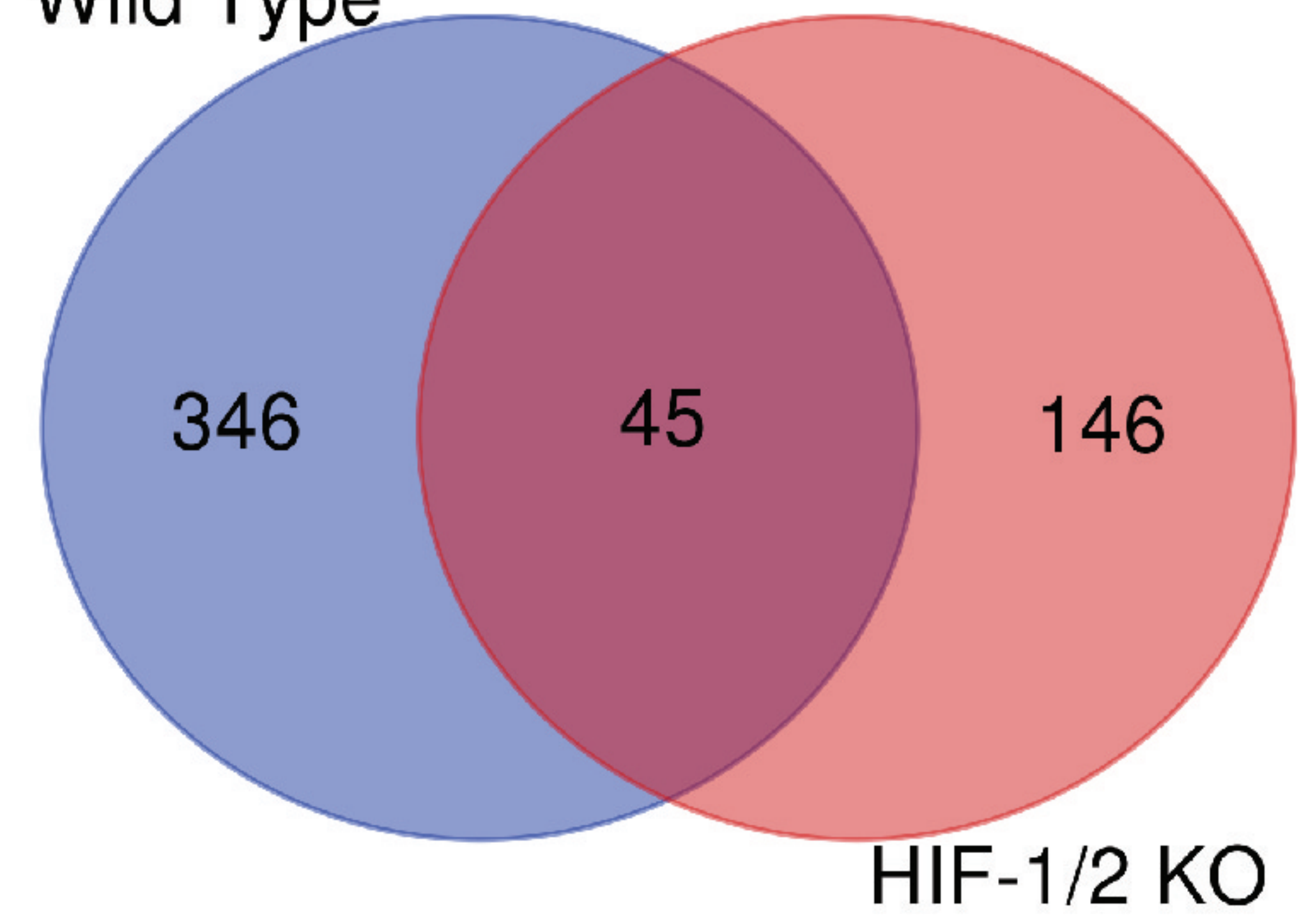
Wild Type



Wild Type



Wild Type



HIF-1 KO

